Original Article

JCBFM

Journal of Cerebral Blood Flow & Metabolism
2017, Vol. 37(5) 1829–1840

DOI: 10.1177/0271678X16659303
journals.sagepub.com/home/jcbfm
SAGE

Requisite ischemia for spreading depolarization occurrence after subarachnoid hemorrhage in rodents

Fumiaki Oka[1,2], Ulrike Hoffmann[1], Jeong Hyun Lee[1], Hwa Kyoung Shin[1], David Y Chung[1,3], Izumi Yuzawa[1], Shih-Pin Chen[1], Yahya B Atalay[1], Ala Nozari[1,4], Kristen Park Hopson[1], Tao Qin[1] and Cenk Ayata[1,3]

Abstract

Spontaneous spreading depolarizations are frequent after various forms of human brain injury such as ischemic or hemorrhagic stroke and trauma, and worsen the outcome. We have recently shown that supply-demand mismatch transients trigger spreading depolarizations in ischemic stroke. Here, we examined the mechanisms triggering recurrent spreading depolarization events for many days after subarachnoid hemorrhage. Despite large volumes of subarachnoid hemorrhage induced by cisternal injection of fresh arterial blood in rodents, electrophysiological recordings did not detect a single spreading depolarization for up to 72 h after subarachnoid hemorrhage. Cortical susceptibility to spreading depolarization, measured by direct electrical stimulation or topical KCl application, was suppressed after subarachnoid hemorrhage. Focal cerebral ischemia experimentally induced after subarachnoid hemorrhage revealed a biphasic change in the propensity to develop peri-infarct spreading depolarizations. Frequency of peri-infarct spreading depolarizations decreased at 12 h, increased at 72 h and normalized at 7 days after subarachnoid hemorrhage compared with sham controls. However, ischemic tissue and neurological outcomes were significantly worse after subarachnoid hemorrhage even when peri-infarct spreading depolarization frequency was reduced. Laser speckle flowmetry implicated cerebrovascular hemodynamic mechanisms worsening the outcome. Altogether, our data suggest that cerebral ischemia is required for spreading depolarizations to be triggered after subarachnoid hemorrhage, which then creates a vicious cycle leading to the delayed cerebral ischemia syndrome.

Keywords

Subarachnoid hemorrhage, delayed cerebral ischemia, spreading depolarization, peri-infarct depolarization, middle cerebral artery occlusion

Received 6 March 2016; Revised 2 June 2016; Accepted 3 June 2016

Introduction

Spreading depolarizations (SD) originate in an apparently spontaneous fashion in the human brain after ischemic, hemorrhagic and traumatic injury.[1] Associated with massive transmembrane ion and water shifts, SDs impose severe metabolic mismatch by increasing the energy demand and reducing blood supply in already critically compromised brain tissue.[2] As a result, SDs expand the injury volume and worsen neurological outcomes.

We have recently shown that in the setting of focal cerebral ischemia, SD waves are triggered when the

[1]Department of Radiology, Massachusetts General Hospital, Charlestown, USA
[2]Department of Neurosurgery, Yamaguchi University School of Medicine, Ube, Japan
[3]Department of Neurology, Massachusetts General Hospital, Boston, USA
[4]Department of Anesthesia, Critical Care & Pain Medicine, Massachusetts General Hospital, Boston, USA

Corresponding author:
Cenk Ayata, Massachusetts General Hospital, 149 13th Street, Charlestown, MA 02129, USA.
Email: cayata@mgh.harvard.edu

supply-demand mismatch in moderately ischemic peri-infarct tissue is transiently worsened either due to increased demand or reduced supply.[3] While this provided a mechanism for SD occurrence in ischemic stroke, mechanisms triggering recurrent SDs days to weeks after subarachnoid hemorrhage (SAH) have been unclear. Previous studies have elegantly demonstrated that elevations in extracellular K^+ concentrations ($[K^+]_e$), when combined with reduced NO availability, evoked an SD event coupled to severe vasoconstriction (i.e. inverse coupling, spreading ischemia) that may form the basis of spontaneous SD occurrence after SAH.[4] Here, we examined spontaneous SD occurrence after experimental SAH in rodents. Our data implicate tissue ischemia as a critical condition for spontaneous SDs to develop after SAH.

Methods

All experimental procedures were carried out in accordance with the ARRIVE guidelines, and the Guide for Care and Use of Laboratory Animals (NIH Publication No. 85-23, 1996), and were approved by the institutional review board (MGH Subcommittee on Research Animal Care [SRAC]). We used male C57BL6J mice (3–4 months age, 25–30 g) or Sprague-Dawley rats (3–4 months age, 300–400 g) in all experiments (Charles River Laboratories, Wilmington, MA, USA). Arterial pH, pO_2, pCO_2, and blood pressure were monitored via a femoral artery catheter and maintained within normal limits (Supplemental Table 1). The rectal temperature was kept at 37 °C using a thermostatic heating pad. Technical failure was the only exclusion criterion, and none was excluded. Where relevant, animals were randomly assigned to experimental groups. Experiments were not carried out in a blinded fashion.

SAH induction

In mice, we induced SAH by single injection of freshly collected homologous arterial blood into the prechiasmatic cistern (pc) or cisterna magna (cm), as reported previously with some modifications.[5] Mice were anesthetized with isoflurane (5% induction, 1% maintenance, in 70% N_2O/30% O_2) and allowed to breathe spontaneously. The head was fixed in a stereotaxic frame. Non-heparinized blood was collected from donor mice of the same vendor, strain, gender, and age. For prechiasmatic cistern SAH (pcSAH), a 0.7-mm burr hole was drilled on the midline 5-mm anterior to bregma. A 27-gauge needle was advanced 5.5 mm at 30 ° angle pointing caudally, and 40 µl blood was injected over 60 s. For cisterna magna SAH (cmSAH), the atlantooccipital membrane was exposed, a 30-gauge needle was inserted horizontally, at 90 ° angle to midline, and 60 µl blood was injected over 45 s. We determined these optimal volumes and injection rates to maximize the survival and the deficits in pilot experiments. In both paradigms, animals were immediately placed in a head-down position for 10 min to facilitate the diffusion of injected blood into the basal cisterns. Controls received physiological saline (pcSal or cmSal) injection. In rats, we used a cmSAH double injection model as reported previously with modifications.[6] Rats were anesthetized with isoflurane (5% induction, 1% maintenance, in 70% N_2O/30% O_2) and allowed to breathe spontaneously. The head was fixed in a stereotaxic frame, atlantooccipital membrane exposed, and a 27-gauge needle inserted at an angle of 45 ° pointing anterior and medially into the cisterna magna. Two hundred microliters of freshly collected autologous non-heparinized arterial blood was then injected over 60 s. After injection, rats were placed prone in a head-down position at a 30 ° angle for 20 min to facilitate the diffusion of injected blood into the basal cisterns. A second bolus of 300 µl was injected 48 h later in a similar fashion. Controls received physiological saline injection. We chose not to use the endovascular perforation method to induce SAH to avoid any inadvertent ischemia and infarction precipitated by the vascular tearing and/or thrombosis that may take place during the perforation procedure, as well as any endothelial disruption and altered cerebrovascular reactivity.

Monitoring spontaneous SD occurrence

We monitored spontaneous SD occurrence electrophysiologically using intracortical glass micropipettes placed 1.5 mm posterior and 2 mm lateral from bregma bilaterally. Extracellular slow potential changes were recorded for a period of 6 h under low dose urethane (500 mg/kg) and isoflurane (0.3%, in 70% N_2/30% O_2) anesthesia, between 3 and 9 h, 12 and 18 h or 72 and 78 h after pcSAH ($n = 4$ in each) or 12 and 18 h after cmSAH ($n = 3$). This anesthetic regimen does not suppress SD susceptibility but is required to maintain a surgical plane.[7] As an additional method to detect SDs, laser speckle flowmetry was used in the same animals to monitor cortical perfusion changes; imaging field was positioned to include both hemispheres. In a separate group of mice, we measured K^+ concentration using a point-of-care device (Horiba, Kyoto, Japan) in 5 µl cerebrospinal fluid (CSF) collected from cisterna magna at 12 and 72 h after pcSAH.

SD triggered by topical blood application

To test whether pial application of normal or acutely hemolyzed arterial blood triggers an SD, all mice were

anesthetized using isoflurane (1.5%, in 70% N_2/30% O_2) and heads fixed in a stereotaxic frame. Arterial blood was collected from donor mice of the same vendor, strain, and age into a heparinized tube. Blood was hemolyzed in a sonicator, and diluted 2, 4, or 8 times by physiological saline. Two burr holes were drilled at (from bregma): 3.5 mm posterior, 2 mm lateral (occipital, 2 mm diameter for KCl application and electric stimulation); 0.5 mm anterior, 1.5 mm lateral (frontal, 1 mm diameter for distal recording site). A cotton ball (1.5 mm diameter) was soaked with normal, undiluted or diluted hemolyzed blood, or KCl solution at concentrations corresponding to undiluted or diluted hemolyzed blood (i.e. 57 mM, 28.5 mM, 14.25 mM, and 7.125 mM, made isotonic by NaCl), placed on the pial surface, and replaced every 10 min 3 times. SD occurrence rate was determined.

SD susceptibility determination

We quantified SD susceptibility 12 and 72 h after pcSAH and 12 h after cmSAH in mice, and 5 days after cmSAH in rats, as described previously.[8,9] All animals were anesthetized using isoflurane (1.5%, in 70% N_2/30% O_2) and fixed in a stereotaxic frame. In mice, three burr holes were drilled at (from bregma): 3.5 mm posterior, 2 mm lateral (occipital, 2 mm diameter for KCl application and electric stimulation); 1.5 mm posterior, 2 mm lateral (parietal, 1 mm diameter for proximal recording site); 0.5 mm anterior, 1.5 mm lateral (frontal, 1 mm diameter for distal recording site). In rats, three burr holes were drilled at (from bregma): 4.5 mm posterior, 2 mm lateral (occipital, 2 mm diameter for electrical stimulation); 1.5 mm posterior, 2 mm lateral (parietal, 1 mm diameter for proximal recording site); 1.5 mm anterior, 2 mm lateral (frontal, 1 mm diameter for distal recording site). For KCl-induced SD susceptibility in mice, we placed a cotton ball (1.5 mm diameter) soaked with 300 mM KCl on the pial surface and kept it moist by placing 5 µl of the same KCl solution every 15 min. The frequency of KCl-induced SDs was calculated. In rats, electric SD threshold was determined by escalating cathodal square pulses (100–4000 microCoulomb, µC) delivered via a bipolar electrode on the occipital pial surface.

Cerebral blood flow response to SD

In a separate cohort, hemodynamic responses to induced SDs were examined at 12 h, 72 h, and 7 days after pcSAH in mice, and 5 days after cmSAH in rats as described previously.[10] Animals were anesthetized with isoflurane (1.5%, in 70% N_2/30% O_2), intubated, mechanically ventilated (SAR830, CWE, Ardmore, PA, USA) and placed on a stereotaxic frame. In mice, cortical perfusion was monitored using laser speckle flowmetry through an intact skull with the imaging field over the right hemisphere.[10] A 1-mm burr hole was drilled over the frontal cortex (2 mm anterior, 1 mm lateral from bregma), and laser speckle flowmetry (LSF) monitoring was started. After baseline imaging for 2 min, an SD was induced by briefly touching a 1-mm diameter cotton ball soaked in 300 mM KCl solution on the prefrontal cortex through the burr hole, immediately followed by careful saline wash. Fifteen minutes later, this procedure was repeated to trigger a second SD. Cerebral blood flow (CBF) changes were calculated for each pixel relative to the pre-SD baseline and the time course of relative CBF was quantified using a region of interest (ROI; 0.25 mm^2) placed within the middle cerebral artery territory avoiding visible pial vessels. Baseline CBF prior to SD induction was estimated using the correlation time value, as previously described,[11] and taken into account when reproducing the CBF time course during and after SD. In rats, cortical perfusion was monitored using laser Doppler flowmetry (LDF) over the parietal cortex. A 1-mm diameter burr hole was drilled over the frontal cortex (2.5 mm anterior, 2 mm lateral from bregma) and an SD was induced by briefly touching a 1-mm diameter cotton ball soaked in 1 M KCl solution on the pial surface, immediately followed by careful saline wash, once in each rat. To accurately represent the multiphasic changes during and after an SD, we measured and averaged across animals the magnitudes and latencies of the following deflection points: baseline, the onset of hypoperfusion, trough, transient normalization, second trough, second rise, and 9, 11, 13, and 15 min after SD onset in mice, and baseline, peak hyperemia, end of hyperemia and 3 and 5 min after SD onset in rats. We then interpolated the averaged deflection points to reconstruct the response to an SD as previously reported.[10,12–14]

Recording peri-infarct SDs

Intraluminal filament occlusion of the middle cerebral artery was carried out as described previously in mice.[9] Under isoflurane (1.5%, in 70% N_2/30% O_2) anesthesia, a silicone-coated 6-0 nylon monofilament was inserted into the internal via the external carotid artery. Occlusion was confirmed using LDF over the ischemic core. To detect peri-infarct SDs, fMCAO was induced at 12 h, 72 h, or 7 days after pcSAH, or 12 h after cmSAH.[9] Mice were immediately transferred to a stereotaxic frame and two 0.5-mm diameter burr holes were drilled at (mm from bregma): 1.5 anterior, 0.5 lateral; 3.5 posterior, 0.5 lateral. These coordinates were reliably outside the ischemic core to allow detection of peri-infarct spreading depolarizations (PIDs).

Two intracortical glass micropipettes were inserted at a depth of 250 µm to record extracellular slow potential changes starting 15 min after the onset of ischemia for approximately 3 h. At the end of PID monitoring, mice were transcardially perfused with heparinized saline, and their brains removed and examined grossly for the amount and distribution of SAH.

Assessment of tissue and neurological outcome after focal ischemia

In a separate cohort, we assessed tissue and neurological outcome 24 h after 30- or 60-min fMCAO followed by reperfusion. Neurological outcomes were scored on a 5-point scale: 0, normal; 1, forepaw monoparesis; 2, circling to left; 3, falling to left; 4, no spontaneous walking and depressed consciousness. Infarct volume was calculated by integrating the ipsilateral non-infarcted area in ten 1-mm-thick 2,3,5-triphenyltetrazolium chloride (TTC)–stained coronal sections, and subtracting its volume from the contralateral hemisphere volume (i.e. indirect infarct).

Imaging the acute ischemic perfusion deficit

We induced distal middle cerebral artery occlusion (dMCAO) at 12 h, 72 h, or 7 days after pcSAH, or 12 h after cmSAH in mice.[15] Under isoflurane (1.5%, in 70% N_2/30% O_2) anesthesia, mice were placed in a stereotaxic frame, temporalis muscle removed, a 2-mm diameter burr hole drilled in the temporal bone overlying the distal MCA just above the zygomatic arch, and distal MCA occluded using a microvascular clip. Cortical perfusion was imaged using LSF through intact skull before, during and after dMCAO. CBF changes were calculated for each pixel relative to the pre-ischemic baseline, and the area of cortex with residual CBF <30% or 30–40% of baseline was determined by thresholding.

Statistics

Statistical analyses were carried out using Prism v 6.0 (GraphPad Software, San Diego, CA, USA). Data were expressed as whisker-bar plots (whisker, full range; bar, interquartile range; line, median; +, mean), or mean ± standard deviation. Statistical tests and sample sizes for each dataset are indicated in the text or figure legends, or directly on the figures. $P < 0.05$ was considered statistically significant.

Results

Twelve hours after pcSAH, large amounts of blood covered the dorsal cortical surface and pial vasculature (Supplemental Figure 1). Gross examination over time revealed persistent albeit reduced presence of blood 3 days after pcSAH, with complete clearance at 7 days. In mice with cmSAH, blood accumulated predominantly in the pre-pontine cistern extending around the circle of Willis, although a thin layer of blood tracked along the perivascular space surrounding the arteries as far as the dorsal cortical surface (Supplemental Figure 2). In contrast to pcSAH, however, blood cleared much faster after cmSAH, becoming undetectable within 24 h.

We monitored spontaneous SD occurrence after pcSAH bilaterally in mice for a cumulative total of 72 h ($n = 4$ mice each between 3 and 9 h, 12 and 18 h, and 72 and 78 h after pcSAH), but did not detect a single spontaneous SD (Figure 1(a)). In three more mice, we monitored SDs 12–18 h after cmSAH (total 18 h of recordings), and once again did not detect any spontaneous SD. This complete absence of spontaneous SDs was in striking contrast to focal cerebral ischemia where numerous SDs consistently occur with high frequency in all species studied to date.[9,16–21] At the end of each experiment, we confirmed the integrity and sensitivity of electrophysiological recordings by inducing and successfully detecting an SD at each recording site in all mice using pinprick (Figure 1(a), dashed arrows).

These data clearly suggested that the presence of dense subarachnoid blood was not sufficient to trigger an SD, even in the highly susceptible mouse cortex. To further confirm this, we tested whether pial application of normal or acutely hemolyzed arterial blood triggered an SD. Topical application of whole non-hemolyzed arterial blood did not trigger SD in any of the experiments. In contrast, acutely hemolyzed undiluted blood triggered an SD 67% of the time (Figure 1(b), left panel). However, this effect was rapidly lost upon stepwise dilution using normal saline, with a concentration–response relationship. We measured the extracellular (i.e. plasma) K^+ concentration ($[K^+]_e$) in undiluted hemolyzed blood and found it to be 57.3 ± 0.3 mM (hemoglobin 1.96 ± 0.07 mM; $n = 3$ independent samples). In separate experiments, we determined the concentration–response relationship between topical KCl solution and SD induction, and found that the ability of hemolyzed blood to trigger SD correlated well with $[K^+]_e$ (Figure 1(b), right panel). These data suggested that K^+ is the main SD trigger in hemolyzed blood, and other substances (e.g. ions, small molecules, peptides) do not significantly contribute. We next measured CSF $[K^+]_e$ after pcSAH in mice but did not detect an increase at any time point (3.7 ± 0.6, 3.4 ± 0.1, and 3.5 ± 0.6 mM, in naïve, and 12 and 72 h after pcSAH, respectively; $n = 3$, 3, and 5), as previously reported.[22–25] This was not surprising because K^+ released into the CSF during gradual lysis of

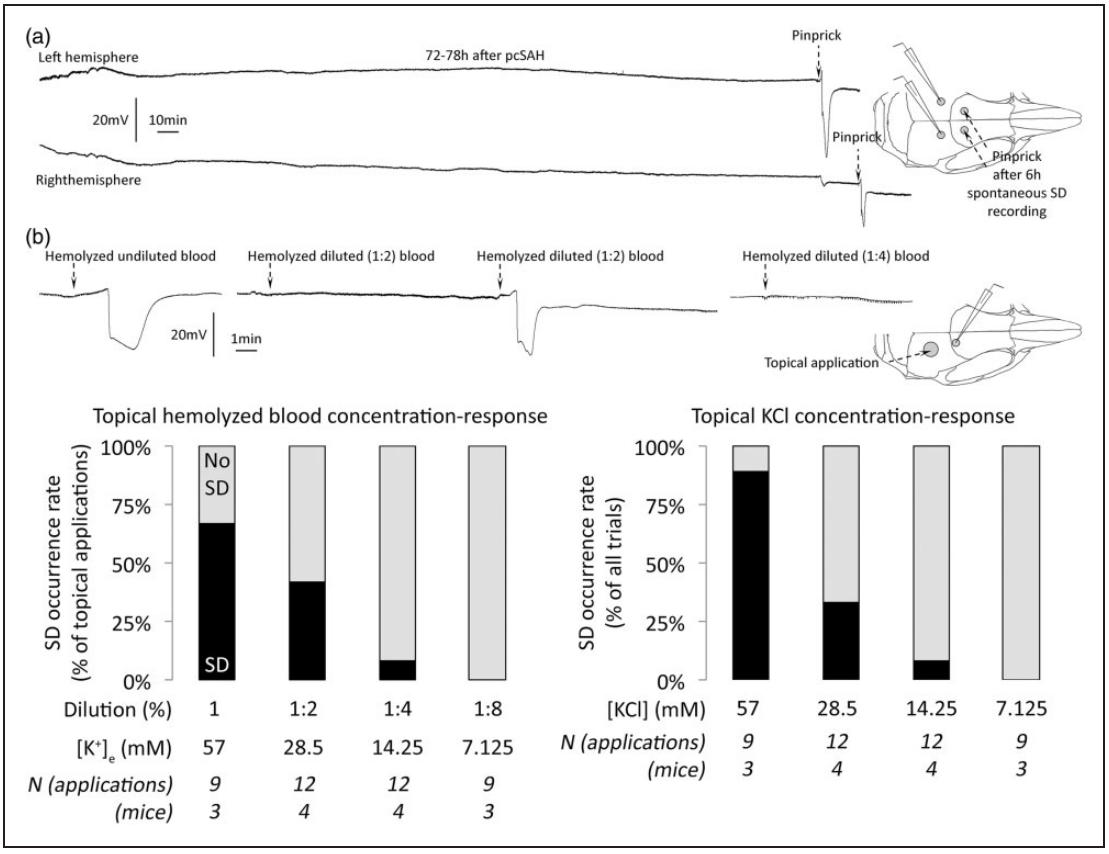

Figure 1. Spontaneous SD occurrence after SAH, and topical blood as a trigger for SD. (a) Extracellular DC potential recordings bilaterally did not detect any spontaneous SD, as shown in these 6-h representative tracings taken between 72 and 78 h after pcSAH. The integrity of the recoding system was confirmed by detection of pinprick-induced SD sequentially in both hemispheres at the end of the monitoring period (dashed arrows). Inset shows electrode positioning. (b) The effect of topical application of hemolyzed blood is shown at different levels of dilution. Representative tracings show the efficacy of undiluted (100%) hemolyzed blood as well as two- (50%) and fourfold (25%) diluted blood to trigger SD upon topical application. Inset shows the electrode positioning and topical application site. Summary data show rapid decline in the efficacy of hemolyzed blood to trigger SD upon successive dilutions (left panel). Black bars show the percentage of all topical applications that triggered an SD at each dilution level. Undiluted hemolyzed blood had a highly consistent 57.3 ± 0.3 mM $[K^+]_e$ (see "Methods" section), which was used to estimate the $[K^+]_e$ of successive dilutions. In a separate cohort, we determined the KCl-concentration response relationship in triggering SD (right panel), and found that the efficacy of hemolyzed blood to trigger SD corresponded well with the efficacy of $[K^+]_e$ in the hemolyzed sample. All KCl solutions were made isotonic by NaCl. Group sizes (N) are indicated under the bars.

subarachnoid blood is likely taken up by astrocytes and neurons and/or otherwise diluted via diffusion and bulk CSF flow. Altogether these data strongly argued against high CSF $[K^+]_e$ as the trigger for spontaneous SDs observed after SAH in human brain.

Next, we tested whether smaller local increases in $[K^+]_e$ or cellular changes after SAH somehow enhance the tissue susceptibility to SD; this might predispose to SDs after SAH under the right conditions. We found no evidence for enhanced SD susceptibility at any of the tested time points after pcSAH or cmSAH in mice, and cmSAH in rats (Figure 2). To the contrary, SD susceptibility was significantly reduced at 12 h after pcSAH or cmSAH in mice, as evident in lower KCl-induced SD frequencies and SD propagation speeds, and normalized within 72 h. Cumulative depolarization durations during continuous topical KCl were also shorter (naïve 366 ± 70 s, 12 h after pcSal 325 ± 101 s, 12 h after pcSAH 228 ± 62 s, 72 h after pcSAH 392 ± 74 s; $p < 0.05$ 12 h after pcSAH vs. all other groups). Similarly, in the rat cmSAH double injection model, electrical SD threshold was significantly elevated at 5 days, and SD propagation speed was reduced. SD duration or amplitude did not show a consistent change (Supplemental Table 2). We selected the 5-day time point in the rat because cmSAH double injection model in this species typically leads to slower onset and longer lasting abnormalities than single injection

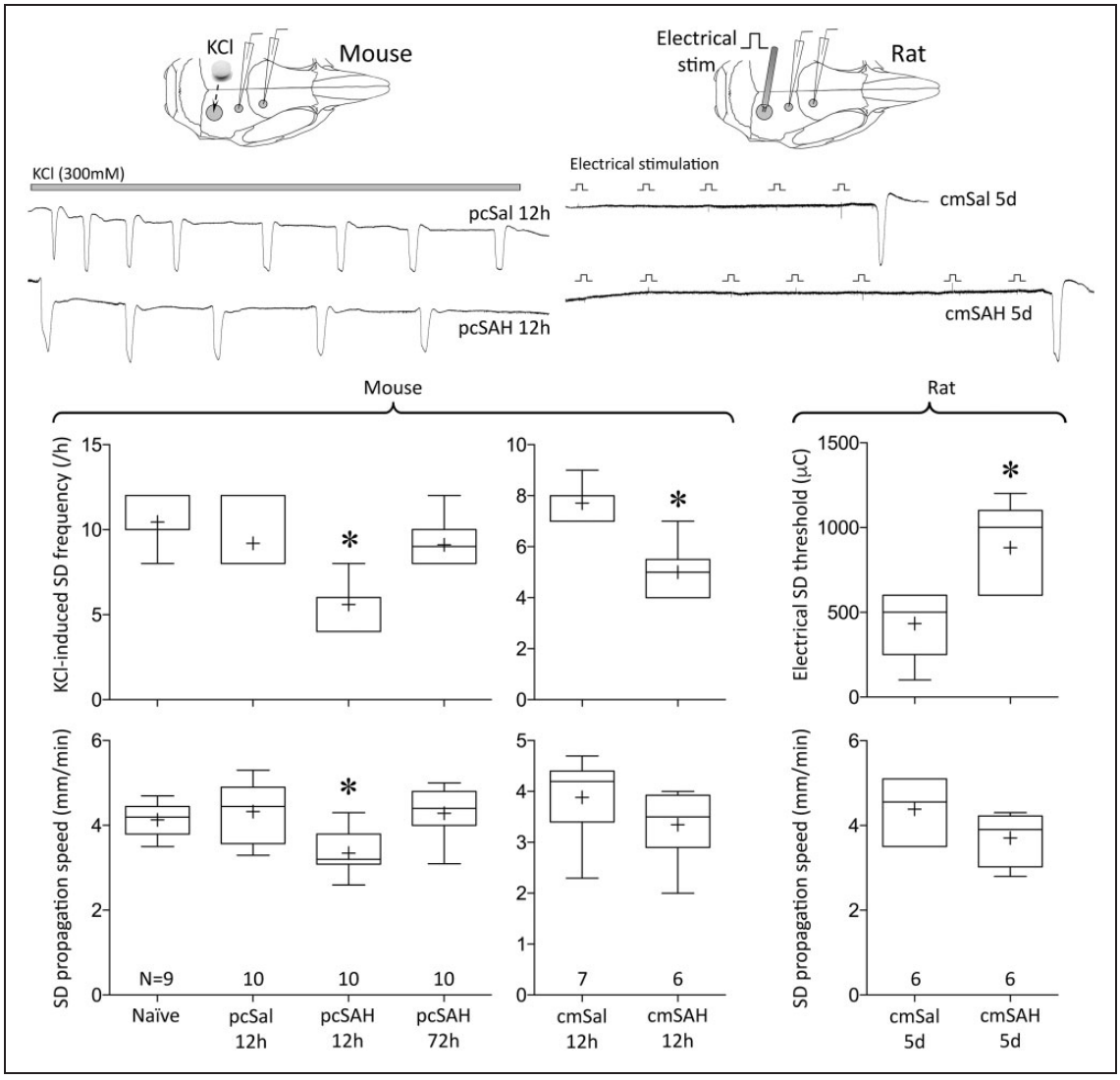

Figure 2. SD susceptibility after SAH. Upper panel shows representative tracings of reduced frequency of repetitive SDs (left) induced by topical KCl (horizontal bar) after pcSAH compared with pcSal in the mouse, and higher threshold for escalating-intensity electrical stimulation-induced SD (right) in cmSAH compared with cmSal in the rat. Insets show the experimental setups. Lower panel shows summary data for SD susceptibility attributes. Group sizes (N) are indicated under the bars. *$p < 0.05$ vs. all other groups; one-way ANOVA (pcSAH) and unpaired t-test (cmSAH).

SAH models in mice. Selected time points, taken together, covered the period of frequent spontaneous SD occurrence after SAH in human brain. These data suggested that the presence of dense subarachnoid blood did not enhance intrinsic SD susceptibility in cortex.

Presence of SAH has been proposed as a mechanism of inverse coupling, where the normally vasodilator, hyperemic response to SD is transformed into a vasoconstrictive hypoperfusion response. Therefore, we tested whether the CBF response to SD is altered after SAH. As a prerequisite for proper interpretation of acute CBF changes during SD, we first measured resting CBF using laser speckle flowmetry and found it to be about 25% and 15% lower than baseline at 12 and 72 h after pcSAH, respectively, in mice; this mild hypoperfusion completely normalized within 7 days (Figure 3(a)). However, we did not observe the typical "spreading ischemia" during SD previously described in the setting of elevated $[K^+]_e$ combined with nitric oxide synthase inhibition to mimic SAH.[27]There were only minor, albeit statistically significant, differences in CBF changes during SD at 12 and 72 h after pcSAH in mice (Figure 3(b)). These changes were largely explained by the reduced resting CBF, which normalized within 7 days. In rats, CBF changes during SD were nearly identical between cmSAH and cmSal (Figure 3(c)). All CBF responses to SD were within

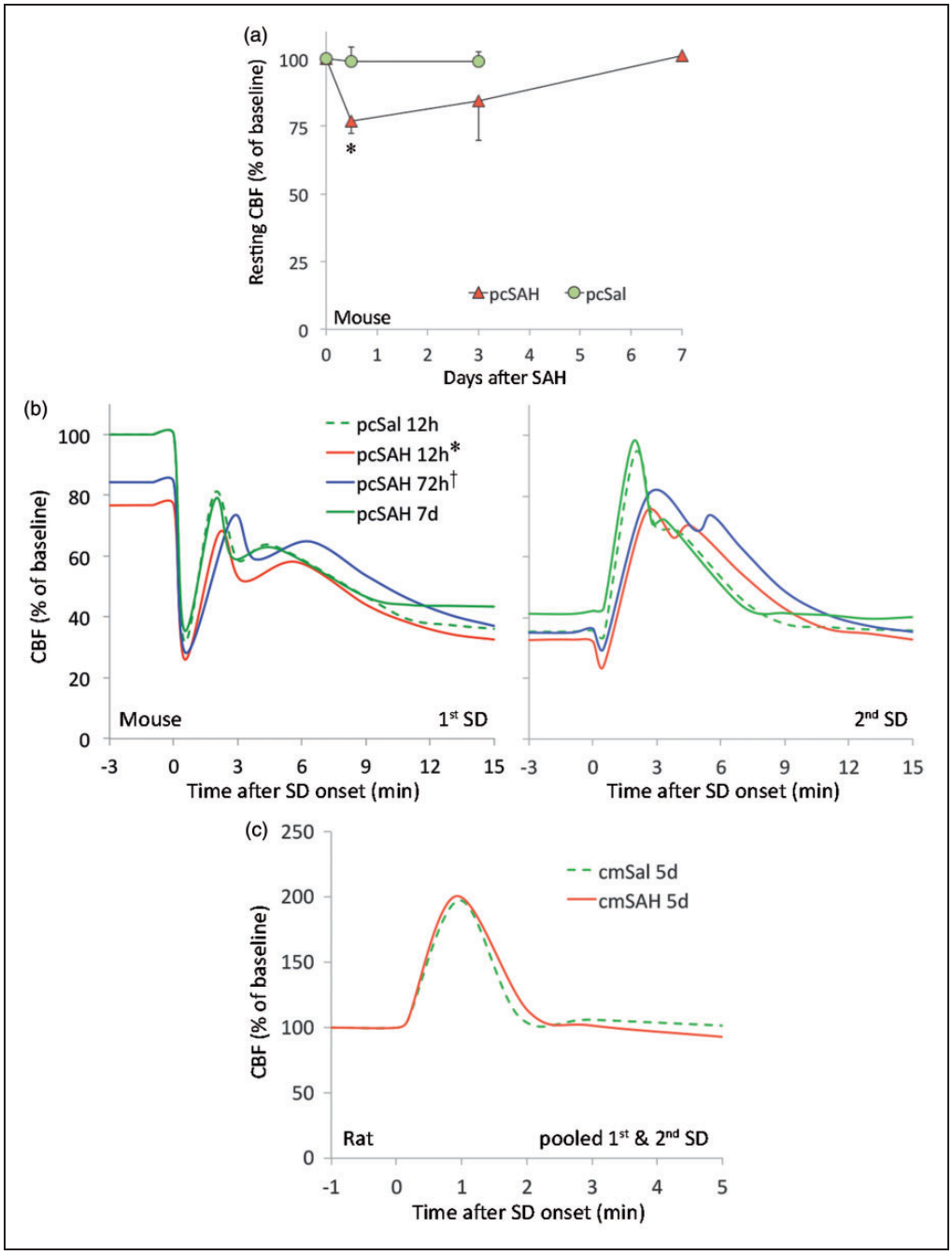

Figure 3. Resting CBF and changes during SD after SAH. (a) Resting CBF was calculated using the correlation time value measured by laser speckle flow imaging, as described previously.[26] Values for each time point after pcSal or pcSAH were obtained in separate groups of mice. Each group was compared with its own baseline by repeat imaging. Compared with baseline, resting CBF decreased by ~25% 12 h after pcSAH and gradually normalized over 7 days (*$p < 0.05$ vs. baseline; two-way repeated measures ANOVA within SAH group). Resting CBF did not change in pcSal group. N = 3 each in pcSal 12 h and 3 days; N = 5, 4, and 3 in pcSAH 12 h, 3 days, and 7 days, respectively. (b) Averaged CBF responses to SD in mice (two consecutive SDs 15 min apart) and rats (single SD). Each SD evoked typical CBF changes as described previously in mice and rats.[2,10,12,13] The pcSal group showed nearly identical CBF responses to SD in naïve mice (not shown). We found only minor, albeit statistically significant differences among the groups in mice (*$p < 0.05$ vs. all other groups in first SD, vs. pcSAH 72 h and 7 days in second SD; †$p < 0.05$ vs. pcSAH 12 h and 7 days in first SD only; two-way repeated measured ANOVA). Majority of the changes could be explained by the reduction in baseline CBF at 12 and 72 h (expressed as % of pre-injection baseline). (c) In rats, CBF response to SD did not differ between cmSal and cmSAH. Error bars were omitted for clarity. N = 5, 7, 5, and 3 mice in pcSal, pcSAH 12 h, pcSAH 72 h, and pcSAH 7 days, respectively. N = 6 rats each cmSal and cmSAH 5 days.

previously reported limits for these species.[2,10,12,28] Altogether, the data did not support the notion that SAH alone radically transforms the cerebral blood flow impact of SDs.

The absence of spontaneous SDs and the normal CBF response to SD after SAH in rodents contrasted sharply with the observations in human brain, where numerous spontaneous SDs and vasoconstrictive (i.e. inverse) hemodynamic response to SDs have been uniformly observed. To explain this paradox, we reasoned that the absence of spontaneous SD events after SAH in rodent brain might be due to milder delayed cerebral ischemia compared with human brain. Hence, we hypothesized that tissue ischemia is a prerequisite for the occurrence of spontaneous SDs and abnormal hemodynamic response to SDs after SAH.

To this end, we induced focal cerebral ischemia at different time points after SAH and examined the peri-infarct SDs and stroke outcome. Occlusion of the middle cerebral artery using an intraluminal filament consistently yielded 4.3 ± 1.2 peri-infarct SDs per hour in pcSal (i.e. control) cohort (pooled data from 12 h, 72 h, and 7 days; $n = 5$, 8, 2, respectively), which did not differ from naïve mice without any subarachnoid injection (3.4 ± 0.9 peri-infarct SDs/h; $n = 5$). In the pcSAH cohort, peri-infarct SD frequency decreased at 12 h (~50% reduction; Figure 4). Identical data were found when cumulative peri-infarct SD duration was calculated instead of peri-infarct SD frequency (348 ± 148, 251 ± 129, 492 ± 117*, 304 ± 130 s depolarization per hour of MCAO per animal; $^*p < 0.05$ vs. pcSAH 12 h). These data were consistent with reduced susceptibility to KCl-induced SDs 12 h after pcSAH as described above (Figure 2). Surprisingly, however, there was a marked increase in peri-infarct SD occurrence when ischemia was induced 72 h after pcSAH (~80% increase, $p < 0.05$). We have not detected any increase in SD susceptibility when induced by topical KCl at 72 h after pcSAH. This effect appeared to be directly related to SAH severity when mice were dichotomized based on the amount of residual subarachnoid blood on postmortem examination (Figure 4(e)). At 7 days, peri-infarct SD frequency was normalized. These data suggested that SAH facilitated peri-infarct SDs in a delayed fashion around 72 h.

We next examined the tissue and neurological outcomes after fMCAO to specifically test whether SAH sensitized the brain to focal ischemic injury. Transient fMCAO for 30 or 60 min yielded significantly larger infarct volumes and worse neurological deficits at 24 h when induced 12 or 72 h after pcSAH, respectively, compared with pcSal (Figure 5(a)). Outcomes did not differ between 12 and 72 h; therefore, focal ischemic outcomes corresponded to subarachnoid blood content rather than peri-infarct SD frequency. Consistent with this, infarcts were also larger when fMCAO was induced 12 but not 24 h after cmSAH compared with cmSal (Figure 5(a)); in this model, subarachnoid blood completely cleared within 24 h. To test whether cerebrovascular dysfunction could explain the worse focal ischemic outcomes after SAH, we next employed laser speckle flow mapping of the perfusion defect during acute distal middle cerebral artery occlusion (dMCAO). The area of cortical perfusion defect almost doubled when dMCAO was induced 12 h after pcSAH, remained significantly larger at 72 h, and normalized at 7 days (Figure 5(b)). The time course of the perfusion defect mirrored resting perfusion changes after pcSAH (Figure 3(a)), rather than the peri-infarct SD frequency (Figure 4). These data implicated cerebral hemodynamic dysfunction as a major mechanism for larger infarcts and worse neurological deficits after fMCAO superimposed on SAH.

Discussion

Our findings challenge the notion that subarachnoid blood breakdown products can directly trigger SDs by way of elevated $[K^+]_e$ or scavenging of NO by hemoglobin. Instead, we propose that focal cerebral ischemia is a prerequisite for SD occurrence after SAH, and that interaction between focal ischemia and SAH creates a vicious cycle (Figure 6). The absence of spontaneous SDs after SAH in mice was likely because delayed cerebral ischemia is typically milder in rodents than human.[29] By superimposing focal ischemia with SAH to better simulate the human condition, we found that the presence of SAH significantly worsens ischemic outcome by disrupting collateral perfusion (12 and 72 h) and facilitating peri-infarct SDs (72 h) in mice. After SAH, focal ischemia can develop via a number of mechanisms such as microvascular plugging due to in situ thrombosis or microembolization.[30] Regardless of the mechanisms precipitating ischemia, SAH-induced vascular dysfunction[31–34] diminishes collateral flow and expands the volume of ischemic tissue. We posit that focal ischemia in turn triggers peri-infarct SDs, facilitated by SAH in a delayed fashion possibly via blood breakdown products or vascular dysfunction. Peri-infarct SDs impose additional metabolic burden, exacerbate vascular dysfunction, and expand the perfusion defect,[2,15,18] particularly when they occur with high frequency and in clusters.[18,35–37] Such a vicious cycle may explain the occurrence and timing of delayed ischemic neurological deficits and infarction (Figure 6).

Peri-infarct SD occurrence showed a biphasic time course after SAH. An early decrease at 12 h was followed by a marked increase at 72 h and normalization at 7 days. The timing of increased peri-infarct SD frequency at 72 h implicates erythrocyte breakdown

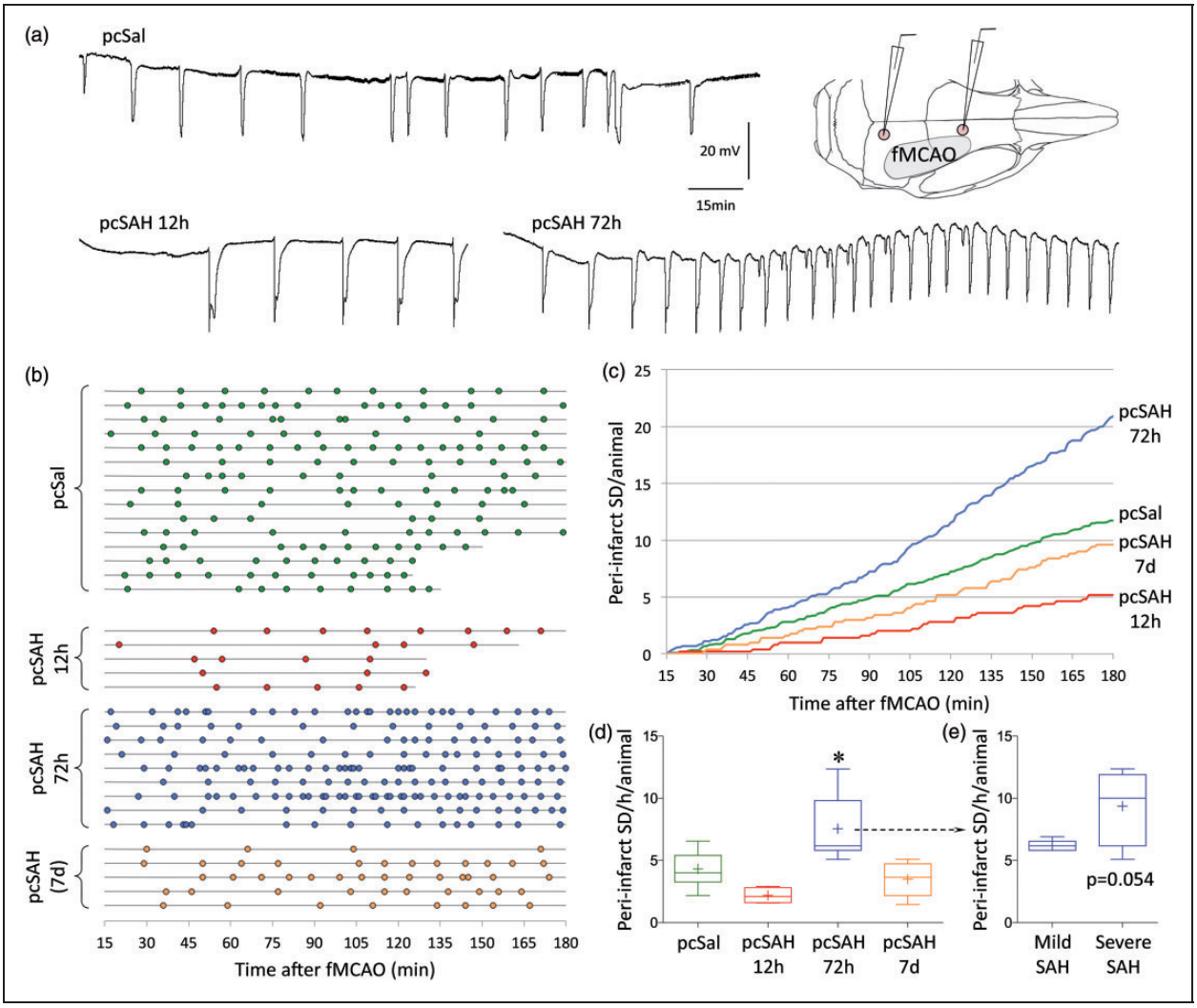

Figure 4. Peri-infarct SDs after SAH. (a) Representative tracings show recurrent peri-infarct SDs after filament middle cerebral artery occlusion (fMCAO) after pcSal, or 12 or 72 h after pcSAH. Inset shows electrode placement in relation to the cortical ischemic territory. (b) Peri-infarct SDs (circles) occurred in all animals and experimental groups throughout the recording period after fMCAO onset. Horizontal lines show the start and end of recording in each animal (n = 15, 5, 9, and 5 mice in pcSal and 12 h, 72 h, and 7-day pcSAH groups, respectively). (c) Cumulative peri-infarct SD occurrence is shown in each experimental group as a function of time. Shorter recordings in a few animals (as shown in (b)) were extrapolated to 180 min based on the average ongoing frequency in that animal. (d) The average hourly frequency of peri-infarct SD occurrence in each animal strongly tended to decrease at 12 h after pcSAH, significantly increased at 72 h, and normalized at 7 days. *$p < 0.05$ vs. all other groups, one-way ANOVA. (e) When we dichotomized the 72-h pcSAH group into mild or severe subarachnoid blood presence based on postmortem examination carried immediately after the electrophysiological recordings, we found a strong trend for the severe SAH subset (n = 4) to develop higher frequency of peri-infarct SDs than the mild SAH subset (n = 5; unpaired t-test).

products, which start by 16–32 h and peak at 7 days.[38] Faster clearance of SAH in rodents compared with human may also explain the normalization of peri-infarct SD frequency at 7 days in our model. The release of intracellular K^+ from ruptured erythrocytes has always been considered a prime candidate as a trigger for SD.[39] Although we did not detect an increase in $[K^+]$ in the CSF collected from the cisterna magna, or spontaneous SDs to suggest that $[K^+]_e$ ever exceeded the SD threshold (~12 mM), small and/or focal elevations in $[K^+]_e$ around the microvasculature and even in the parenchyma[40] might still facilitate peri-infarct SD occurrence. Not consistent with this notion, however, is the lack of an increase in KCl- or electrically induced SD susceptibility at any time point after SAH in mice or rats. Alternatively, increased peri-infarct SD frequency at 72 h may simply reflect larger volumes of ischemic tissue, since larger infarcts naturally trigger more peri-infarct SDs.[21] However, the volume of ischemic tissue was equally large at 12 h,

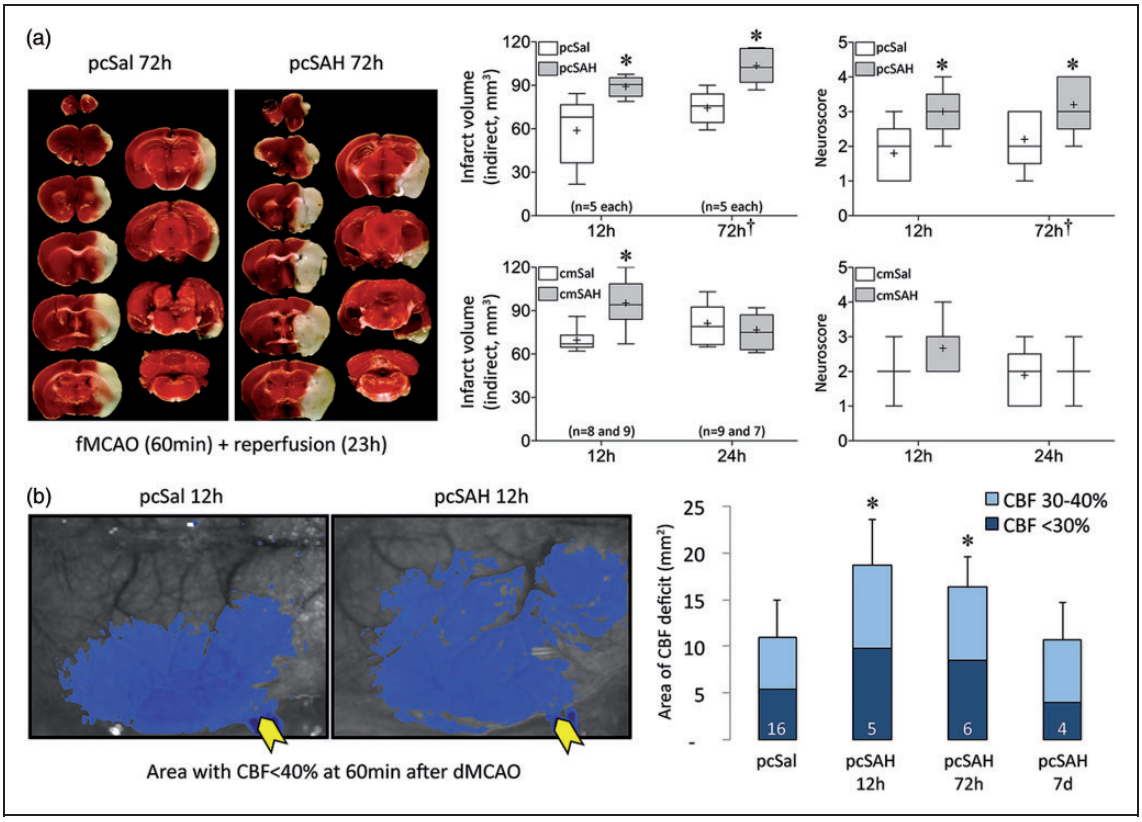

Figure 5. Tissue and neurological outcomes and perfusion defect after focal cerebral ischemia induced at different time points after SAH. (a) Representative, TTC-stained, 1-mm thick coronal sections show the infarct (white tissue) 23 h after 60-min transient fMCAO induced 72 h after pcSal or pcSAH. Summary of tissue outcomes and neurological deficit scores are shown on the right. *$p < 0.05$ vs. pcSal; two-way ANOVA. In 12-h pcSAH and pcSal groups, we used 30-min fMCAO to minimize mortality; in all subsequent experiments, we used 60-min fMCAO. As a result, overall outcomes were worse in 72-h compared with 12-h group (†$p < 0.05$ vs. 12 h). Mortality was 1 in pcSAH 72 h, 3 in cmSal 12 h, 2 in cmSAH 12 h, and 2 in cmSAH 24 h. These are not included in the group sizes indicated on the figure. The volume of ischemic brain swelling (i.e. ipsilateral – contralateral hemisphere volume) did not differ between saline and SAH groups (data not shown). Group sizes are indicated under the bars. (b) Representative laser speckle flowmetry images of dorsal right hemisphere (upper panel) show the perfusion defect (residual CBF < 40% of pre-ischemic baseline, blue pixels) induced by dMCAO performed 12 h after pcSal or pcSAH. Yellow arrows point to the microvascular clip at the occlusion site. Lower panel shows averaged data using two different thresholding levels indicating moderate (light blue) and severe (dark blue) ischemia, respectively. *$p < 0.05$ vs. pcSal. Group sizes are indicated on the bars.

yet peri-infarct SD frequency was decreased rather than increased. Mechanisms of reduced SD susceptibility and peri-infarct SD frequency at 12 h after pcSAH and cmSAH in mice, and 5 days after cmSAH in rats, were also not clear. A similar trend has recently been reported 1 day after endovascular perforation model of SAH in the rat.[41] We have previously shown that mild hypoperfusion induced by bilateral carotid stenosis reduces KCl-induced SD frequency; however, this was consistently associated with significantly prolonged SD durations, which we did not detect after SAH (Supplemental Table 2).[42] Astrocytic and microglial activation may be an alternative mechanism that can suppress SD susceptibility,[43] although their time course in our SAH models remains to be determined. Last, it should be noted that acute SAH likely triggers one or more SDs within seconds to minutes after aneurysmal rupture, perhaps due to global ischemia during the intracranial pressure rise. Acute experimental SAH does indeed elevate local $[K^+]_e$ in cats, which starts within seconds and lasts a few minutes.[44,45] The mechanism may involve local pressure build up or acute perfusion drop. These acute changes, however, cannot explain the delayed occurrence of recurrent SDs for many days after SAH.

In summary, we show that elevated $[K^+]_e$ by itself is not sufficient to explain SD occurrence after SAH. Our data suggest that focal cerebral ischemia is a critical determinant of SD occurrence, and reciprocal interactions between focal cerebral ischemia and SAH

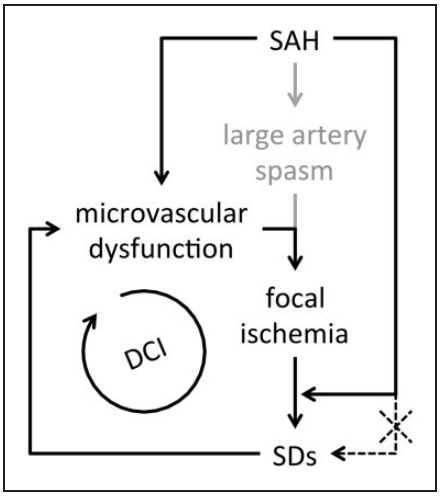

Figure 6. Proposed mechanism in which focal ischemia is a prerequisite for SDs after SAH. Vicious cycle created by focal ischemia, SDs and microvascular dysfunction after SAH lead to delayed cerebral ischemia and infarction (DCI). SAH alone is insufficient to directly trigger SDs (dashed line).

synergize to create a vicious cycle and facilitate injury, leading to the syndrome of delayed cerebral ischemia (DCI). Similar ischemic triggers may underlie SD occurrence in traumatic brain injury and intracerebral hemorrhage as well. Based on these findings, we speculate that antithrombotic therapies, when safe to implement after SAH (e.g. aneurysm clipping), might prevent microvascular occlusion and peri-infarct SD occurrence after SAH to break the vicious cycle.

Funding

The author(s) disclosed receipt of the following financial support for the research, authorship, and/or publication of this article: Supported by grants from the Japanese Heart Foundation/Bayer Yakuhin Research Grant Abroad, NIH (NS055104, NS061505), the Fondation Leducq, the Heitman Foundation, and the Ellison Foundation.

Declaration of conflicting interests

The author(s) declared no potential conflicts of interest with respect to the research, authorship, and/or publication of this article.

Authors' contributions

FO, UH, JHL, HKS, DC, IY, SPC, YBA, AN, KPH, and TQ performed the experiments, analyzed the data and revised the manuscript; CA conceived the study, analyzed the data, and wrote the manuscript.

Supplementary material

Supplementary material for this paper can be found at http://jcbfm.sagepub.com/content/by/supplemental-data

References

1. Lauritzen M, Dreier JP, Fabricius M, et al. Clinical relevance of cortical spreading depression in neurological disorders: migraine, malignant stroke, subarachnoid and intracranial hemorrhage, and traumatic brain injury. *J Cereb Blood Flow Metab* 2011; 31: 17–35.
2. Ayata C and Lauritzen M. Spreading depression, spreading depolarizations, and the cerebral vasculature. *Physiol Rev* 2015; 95: 953–993.
3. von Bornstadt D, Houben T, Seidel JL, et al. Supply-demand mismatch transients in susceptible peri-infarct hot zones explain the origins of spreading injury depolarizations. *Neuron* 2015; 85: 1117–1131.
4. Dreier JP. The role of spreading depression, spreading depolarization and spreading ischemia in neurological disease. *Nat Med* 2011; 17: 439–447.
5. Sabri M, Jeon H, Ai J, et al. Anterior circulation mouse model of subarachnoid hemorrhage. *Brain Res* 2009; 1295: 179–185.
6. Vatter H, Weidauer S, Konczalla J, et al. Time course in the development of cerebral vasospasm after experimental subarachnoid hemorrhage: clinical and neuroradiological assessment of the rat double hemorrhage model. *Neurosurgery* 2006; 58: 1190–1197; discussion 1190–1197.
7. Kudo C, Nozari A, Moskowitz MA, et al. The impact of anesthetics and hyperoxia on cortical spreading depression. *Exp Neurol* 2008; 212: 201–206.
8. Ayata C, Jin H, Kudo C, et al. Suppression of cortical spreading depression in migraine prophylaxis. *Ann Neurol* 2006; 59: 652–661.
9. Eikermann-Haerter K, Lee JH, Yalcin N, et al. Migraine prophylaxis, ischemic depolarizations, and stroke outcomes in mice. *Stroke* 2015; 46: 229–236.
10. Yuzawa I, Sakadzic S, Srinivasan VJ, et al. Cortical spreading depression impairs oxygen delivery and metabolism in mice. *J Cereb Blood Flow Metab* 2012; 32: 376–386.
11. Shin HK, Jones PB, Garcia-Alloza M, et al. Age-dependent cerebrovascular dysfunction in a transgenic mouse model of cerebral amyloid angiopathy. *Brain* 2007; 130(Pt 9): 2310–2319.
12. Ayata C, Shin HK, Salomone S, et al. Pronounced hypoperfusion during spreading depression in mouse cortex. *J Cereb Blood Flow Metab* 2004; 24: 1172–1182.
13. Sukhotinsky I, Dilekoz E, Moskowitz MA, et al. Hypoxia and hypotension transform the blood flow response to cortical spreading depression from hyperemia into hypoperfusion in the rat. *J Cereb Blood Flow Metab* 2008; 28: 1369–1376.
14. Hoffmann U, Sukhotinsky I, Atalay YB, et al. Increased glucose availability does not restore prolonged spreading depression durations in hypotensive rats without brain injury. *Exp Neurol* 2012; 238: 130–132.
15. Shin HK, Dunn AK, Jones PB, et al. Vasoconstrictive neurovascular coupling during focal ischemic depolarizations. *J Cereb Blood Flow Metab* 2006; 26: 1018–1030.
16. Fabricius M, Fuhr S, Bhatia R, et al. Cortical spreading depression and peri-infarct depolarization in acutely

injured human cerebral cortex. *Brain* 2006; 129(Pt 3): 778–790.
17. D'Arceuil HE and de Crespigny A. Dynamic diffusion magnetic resonance imaging of infarct formation and peri-infarct spreading depression after Middle Cerebral Artery Occlusion (MCAO) in macacca fasicularis. *Open Neuroimag J* 2011; 5: 153–159.
18. Strong AJ, Anderson PJ, Watts HR, et al. Peri-infarct depolarizations lead to loss of perfusion in ischaemic gyrencephalic cerebral cortex. *Brain* 2007; 130(Pt 4): 995–1008.
19. Luckl J, Zhou C, Durduran T, et al. Characterization of periinfarct flow transients with laser speckle and Doppler after middle cerebral artery occlusion in the rat. *J Neurosci Res* 2009; 87: 1219–1229.
20. Hartings JA, Rolli ML, Lu XC, et al. Delayed secondary phase of peri-infarct depolarizations after focal cerebral ischemia: relation to infarct growth and neuroprotection. *J Neurosci* 2003; 23: 11602–11610.
21. Eikermann-Haerter K, Lee JH, Yuzawa I, et al. Migraine mutations increase stroke vulnerability by facilitating ischemic depolarizations. *Circulation* 2012; 125: 335–345.
22. Mori K. Double cisterna magna blood injection model of experimental subarachnoid hemorrhage in dogs. *Transl Stroke Res* 2014; 5: 647–652.
23. Wilkins RH and Levitt P. Potassium and the pathogenesis of cerebral arterial spasm in dog and man. *J Neurosurg* 1971; 35: 45–50.
24. Wolf EW, Banerjee A, Soble-Smith J, et al. Reversal of cerebral vasospasm using an intrathecally administered nitric oxide donor. *J Neurosurg* 1998; 89: 279–288.
25. Sambrook MA, Hutchinson EC and Aber GM. Metabolic studies in subarachnoid haemorrhage and strokes. II. Serial changes in cerebrospinal fluid and plasma urea electrolytes and osmolality. *Brain* 1973; 96: 191–202.
26. Ayata C, Shin HK, Dilekoz E, et al. Hyperlipidemia disrupts cerebrovascular reflexes and worsens ischemic perfusion defect. *J Cereb Blood Flow Metab* 2013; 33: 954–962.
27. Dreier JP, Major S, Manning A, et al. Cortical spreading ischaemia is a novel process involved in ischaemic damage in patients with aneurysmal subarachnoid haemorrhage. *Brain* 2009; 132(Pt 7): 1866–1881.
28. Hoffmann U and Ayata C. Neurovascular coupling during spreading depolarizations. *Acta Neurochir Suppl* 2013; 115: 161–165.
29. Megyesi JF, Vollrath B, Cook DA, et al. In vivo animal models of cerebral vasospasm: a review. *Neurosurgery* 2000; 46: 448–460; discussion 460–461.
30. Macdonald RL. Delayed neurological deterioration after subarachnoid haemorrhage. *Nat Rev Neurol* 2014; 10: 44–58.
31. Koide M, Bonev AD, Nelson MT, et al. Inversion of neurovascular coupling by subarachnoid blood depends on large-conductance Ca2+-activated K + (BK) channels. *Proc Natl Acad Sci USA* 2012; 109: E1387–E1395.
32. McConnell ED, Wei HS, Reitz KM, et al. Cerebral microcirculatory failure after subarachnoid hemorrhage is reversed by hyaluronidase. *J Cereb Blood Flow Metab* 2016; 36(9): 1537–1552.
33. Jakubowski J, Bell BA, Symon L, et al. A primate model of subarachnoid hemorrhage: change in regional cerebral blood flow, autoregulation carbon dioxide reactivity, and central conduction time. *Stroke* 1982; 13: 601–611.
34. Schmieder K, Moller F, Engelhardt M, et al. Dynamic cerebral autoregulation in patients with ruptured and unruptured aneurysms after induction of general anesthesia. *Zentralblatt fur Neurochirurgie* 2006; 67: 81–87.
35. Back T, Kohno K and Hossmann KA. Cortical negative DC deflections following middle cerebral artery occlusion and KCl-induced spreading depression: effect on blood flow, tissue oxygenation, and electroencephalogram. *J Cereb Blood Flow Metab* 1994; 14: 12–19.
36. Dohmen C, Sakowitz OW, Fabricius M, et al. Spreading depolarizations occur in human ischemic stroke with high incidence. *Ann Neurol* 2008; 63: 720–728.
37. Dreier JP, Woitzik J, Fabricius M, et al. Delayed ischaemic neurological deficits after subarachnoid haemorrhage are associated with clusters of spreading depolarizations. *Brain* 2006; 129(Pt 12): 3224–3237.
38. Macdonald RL and Weir BK. A review of hemoglobin and the pathogenesis of cerebral vasospasm. *Stroke* 1991; 22: 971–982.
39. Dreier JP, Korner K, Ebert N, et al. Nitric oxide scavenging by hemoglobin or nitric oxide synthase inhibition by N-nitro-L-arginine induces cortical spreading ischemia when K + is increased in the subarachnoid space. *J Cereb Blood Flow Metab* 1998; 18: 978–990.
40. Ohta T, Osaka K, Siguma M, et al. *Cerebral vasospasm following ruptured intracranial aneurysm, especially some contributions of potassium ion released from subarachnoid hematoma to delayed cerebral vasospasm*. New York: Raven Press, 1983.
41. Hamming AM, Wermer MJ, Umesh Rudrapatna S, et al. Spreading depolarizations increase delayed brain injury in a rat model of subarachnoid hemorrhage. *J Cereb Blood Flow Metab* 2016; 36: 1224–1231.
42. Eikermann-Haerter K, Yuzawa I, Dilekoz E, et al. Cerebral autosomal dominant arteriopathy with subcortical infarcts and leukoencephalopathy syndrome mutations increase susceptibility to spreading depression. *Ann Neurol* 2011; 69: 413–418.
43. Sukhotinsky I, Dilekoz E, Wang Y, et al. Chronic daily cortical spreading depressions suppress spreading depression susceptibility. *Cephalalgia* 2011; 31: 1601–1608.
44. Hubschmann OR and Kornhauser D. Effect of subarachnoid hemorrhage on the extracellular microenvironment. *J Neurosurg* 1982; 56: 216–221.
45. Hubschmann OR and Kornhauser D. Cortical cellular response in acute subarachnoid hemorrhage. *J Neurosurg* 1980; 52: 456–462.